Mass spectrometry imaging and ultrasensitive analysis of biological samples on nanophotonic laser desorption ionization platforms

THE GEORGE WASHINGTON UNIVERSITY WASHINGTON, DC

Sylwia A. Stopka,[a] Andrew R. Korte,[a] Charles Rong,[a] Trust T. Razunguzwa,[b] Nicholas J. Morris,[b] Scott T. Retterer,[c] and Akos Vertes[a]

[a]Department of Chemistry, W. M. Keck Institute for Proteomics Technology and Applications, The George Washington University, Washington, DC 20052
[b]Protea Biosciences Inc., 1311 Pineview Drive, Suite 501, Morgantown, WV, 26505
[c]Center for Nanophase Materials Sciences and Biosciences Division, Oak Ridge National Laboratory, Oak Ridge, Tennessee, TN, 37831

INTRODUCTION

- Mass spectrometry imaging (MSI) provides valuable information on the distribution of biomolecules and xenobiotics in biological tissues.
- A main method for MSI is matrix assisted laser desorption ionization (MALDI). However, matrices can interfere with the analysis of small molecules, and their varying crystal sizes and limited uniformity can degrade the image quality.
- Matrix-free laser desorption ionization (LDI) platforms, such as silicon nanopost arrays (NAPA), have demonstrated ultra-trace analysis of volume-limited samples, including single biological cells, with a limit of detection of 800 zmol.[1]
- Here we present the first LDI imaging experiments from NAPA platforms, and the introduction of elevated bowtie (EBT) antenna arrays to enhance ultra-trace analysis from NAPA.

METHODS

- The nanofabrication of NAPA platforms and EBT consisted of deep-UV projection lithography and e-beam lithography, respectively, followed by reactive ion etching.
- Brain and kidney tissues were obtained from healthy adult mice and sectioned at -23°C to a thickness of 10 µm. *Chlamydomonas reinhardtii* cells were cultured in tris-acetate phosphate medium at 27°C.
- Minimal sample preparation included transferring the sectioned tissue onto the NAPA platform, following by vacuum drying at ~800 mbar and mounting the platform directly onto a MALDI plate for LDI-MS analysis, all within ~5 min. The workflow is shown in Figure 1.
- Imaging and ultra-trace analysis were performed using a MALDI LTQ Orbitrap XL mass spectrometer with a 50 µm lateral resolution. The laser fluence and number of shots were dependent on the sample type and fell within 8-100 mJ/cm² and 2-10 pulses, respectively.

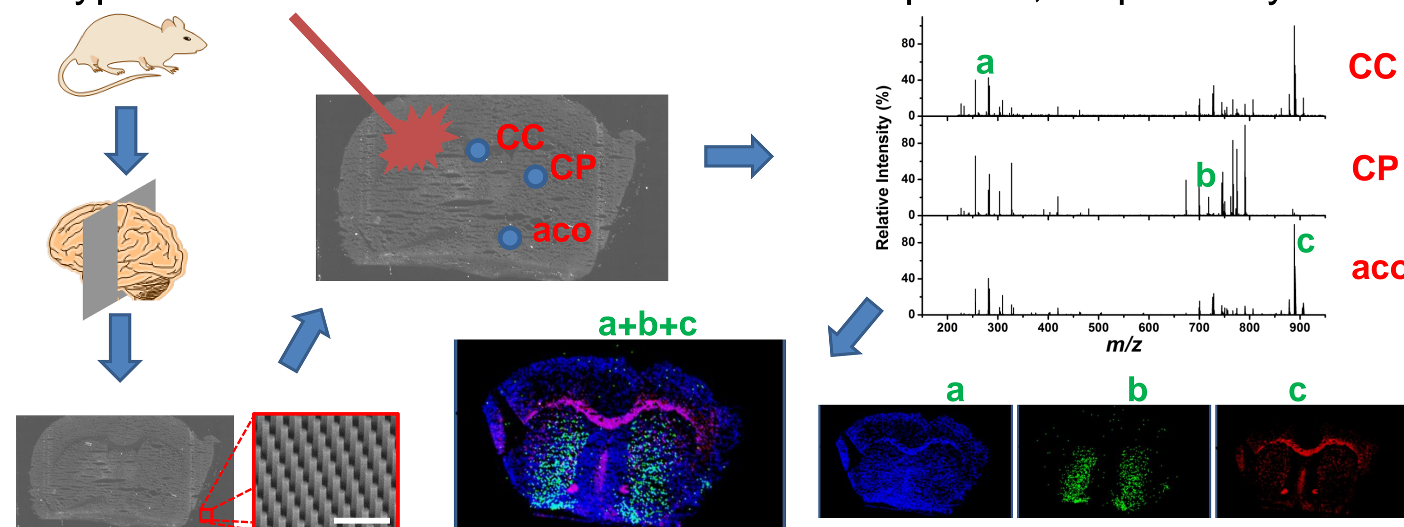

Figure 1. Schematic representation of the workflow for LDI-MSI from NAPA for biological tissue sections.

RESULTS

NAPA-LDI MOUSE BRAIN IMAGING

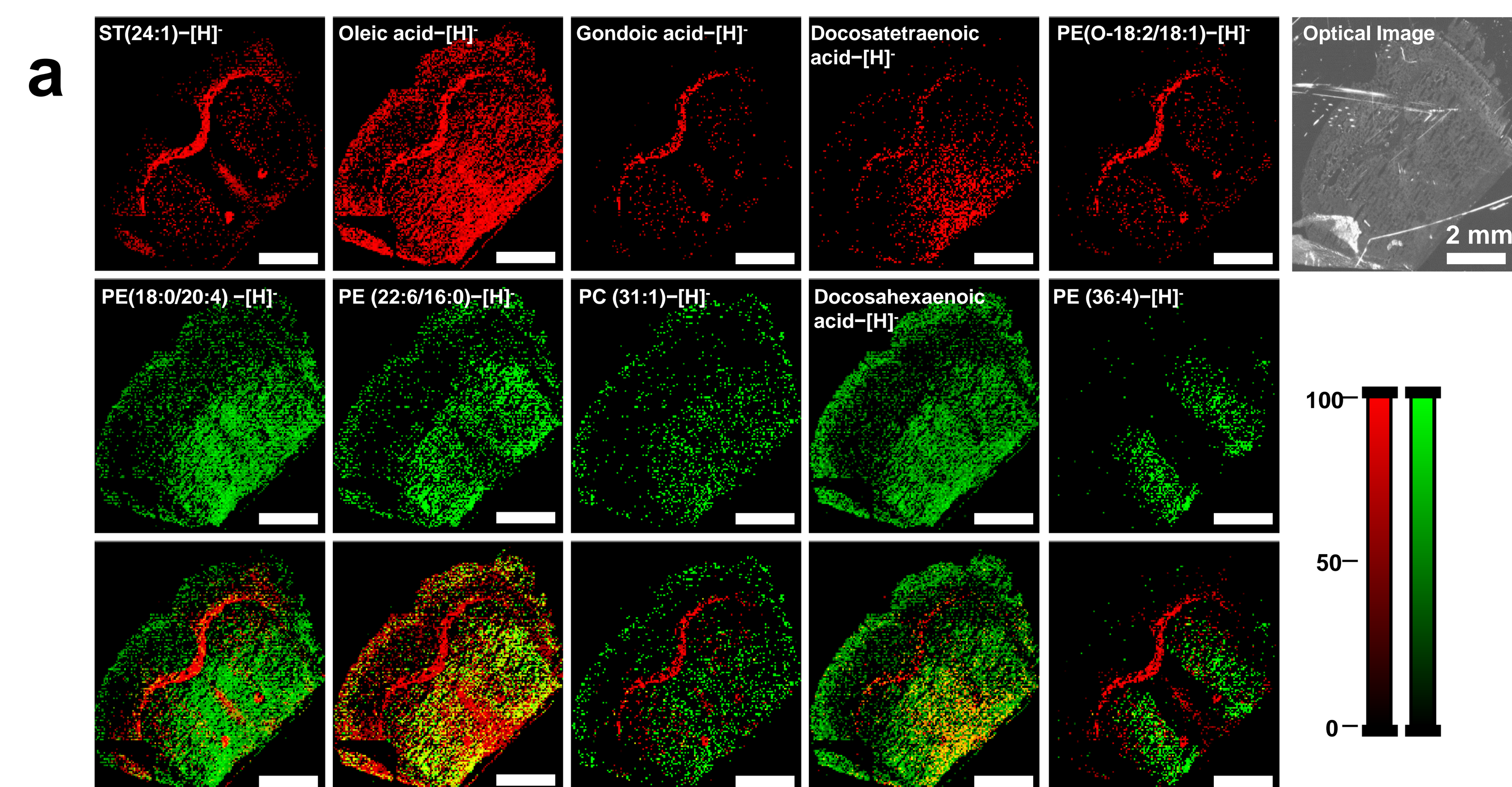

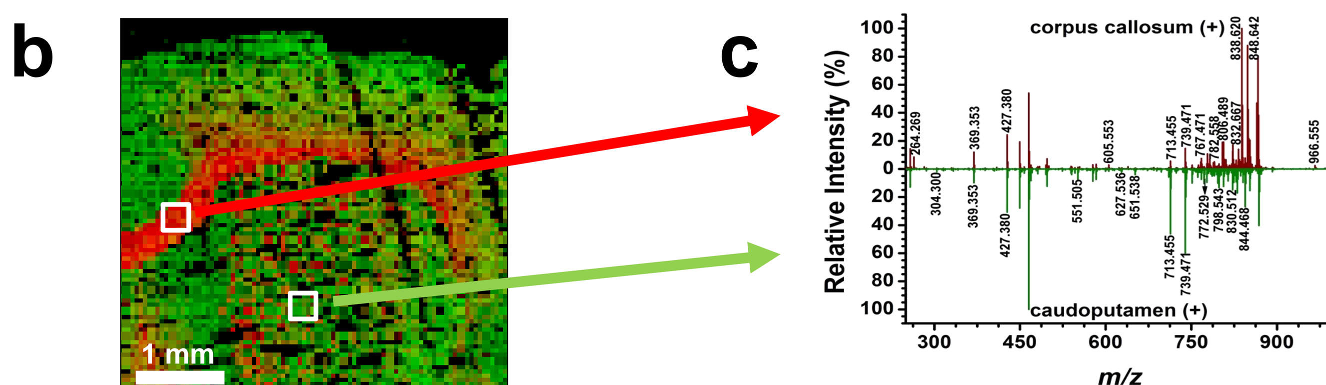

Figure 2. **(a)** Lipid and fatty acid distributions (top and middle), and composite plots (bottom) in coronal mouse brain sections imaged by negative ion LDI-MS from NAPA. **(b)** Coronal mouse brain section composite image by positive ion LDI-MS from NAPA for *m/z* 848.6424 (red) and *m/z* 739.4719 (green) showed localization in anatomically distinct regions. **(c)** Mass spectra from the corpus callosum (CC) (red) and caudoputamen (CP) (green) exhibited region-specific chemical species.

NAPA-LDI MOUSE KIDNEY IMAGING

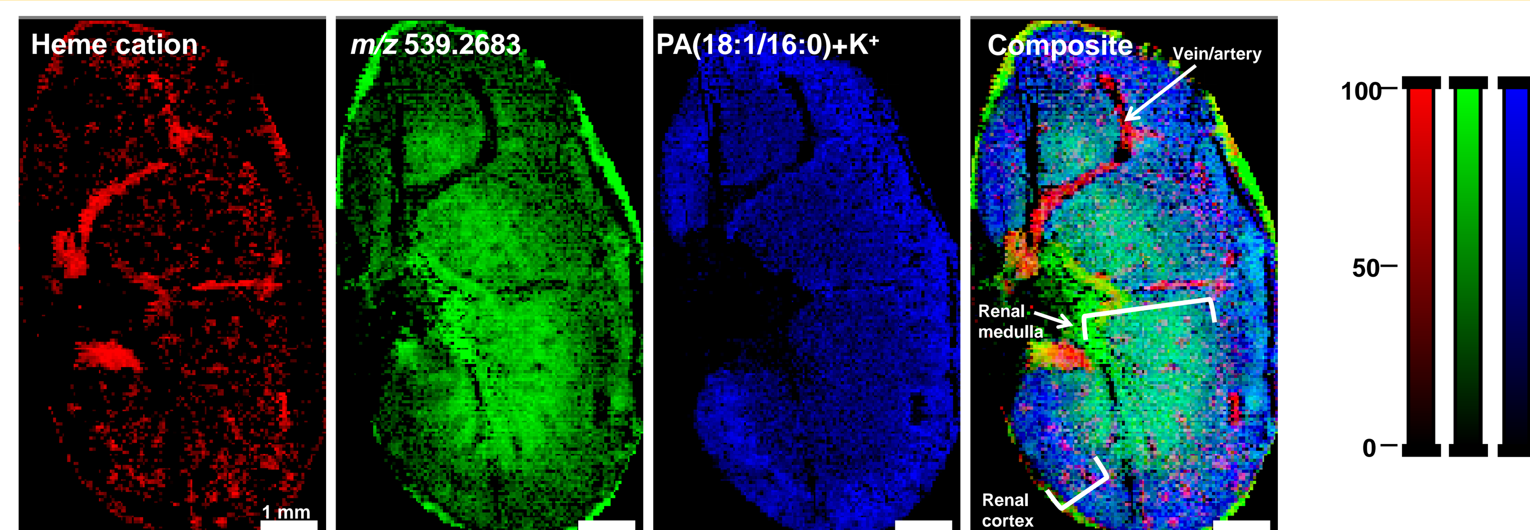

Figure 3. Three ion distributions and composite plot for sagittal mouse kidney section by positive ion LDI-MS imaging from NAPA. Region-specific ions were detected corresponding to anatomical features including the rental cortex and medulla.

SMALL CELL POPULATIONS

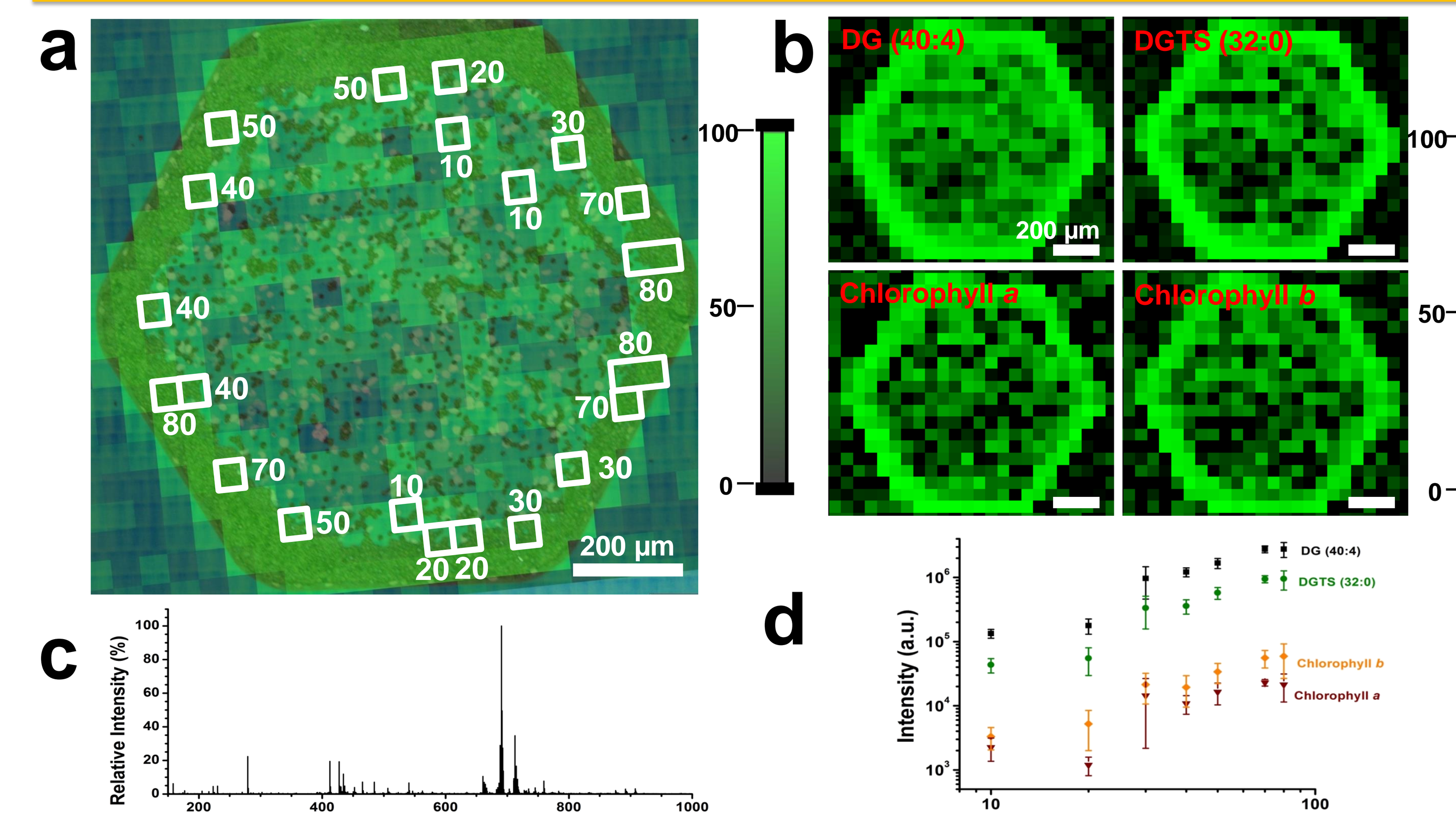

Figure 4. Analysis of small cell populations as a function of cluster size and localization is demonstrated by LDI-MS imaging of *C. reinhardtii* cells on a NAPA platform. **(a)** DG(40:4) chemical image overlaid on an optical image. Each 50 µm MSI pixel corresponds to a specific number of cells as indicated. **(b)** The NAPA-LDI images of four different ions correlating ion intensities in a pixel with cell numbers. **(c)** Mass spectrum of 50 cells analyzed by NAPA-LDI at 60 mJ/cm² laser energy from a single pixel. **(d)** Ion intensities are proportional with cell numbers within the 20 to 100 cell range.

ELEVATED BOWTIE ANTENNA ARRAYS

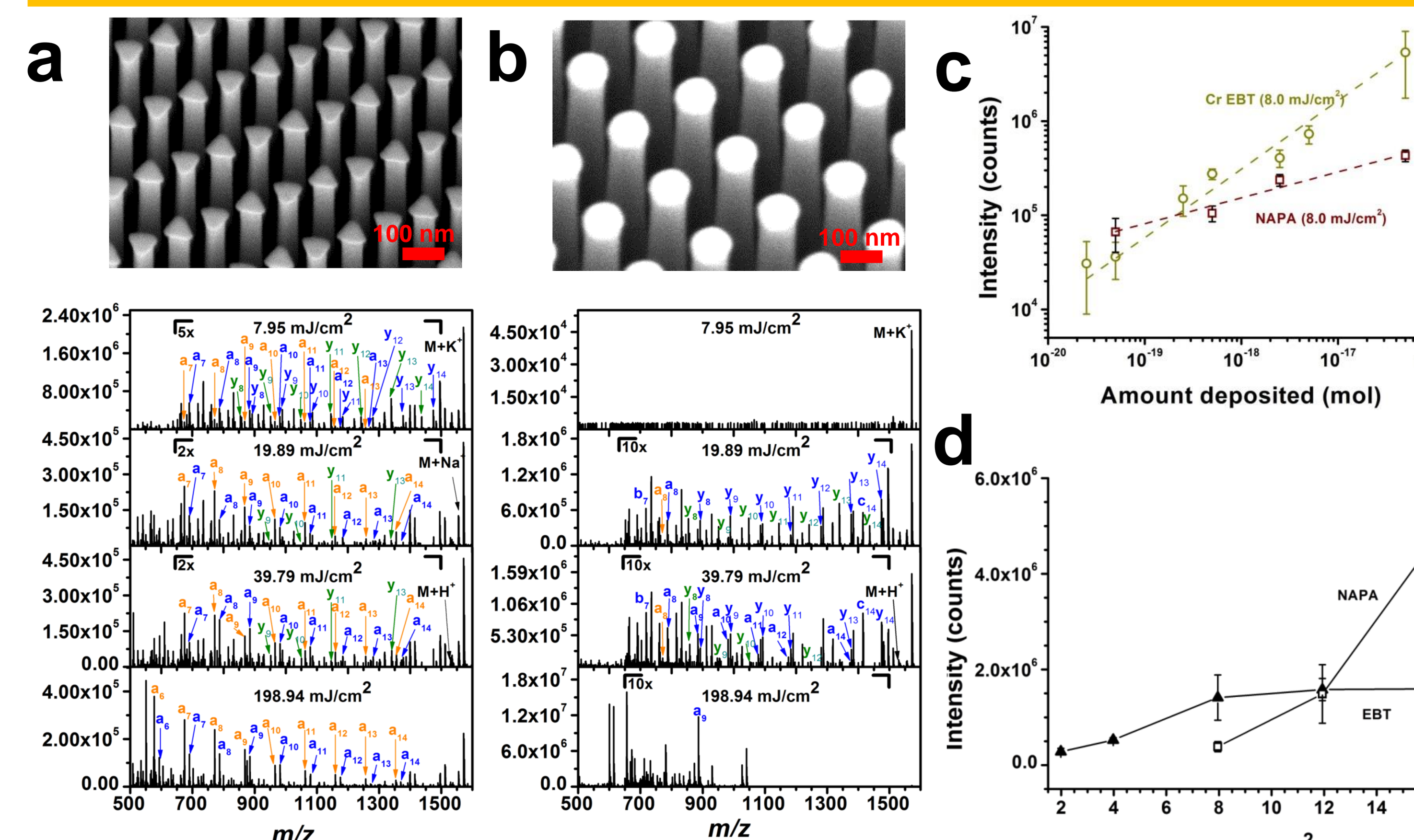

Figure 5. Compared to NAPA, LDI-MS from EBT exhibited enhanced signal intensities at lower fluence thresholds for ionization and fragmentation. **(a)** and **(b)** Comparison of SEM images and in-source fragmentation of the $P_{14}R$ peptide at increasing fluences for LDI from EBT and NAPA, indicated fragmentation by (green) H⁺, (orange) Na⁺, and (blue) K⁺ adducts. **(c)** Limit of detection and dynamic range for verapamil from EBT and NAPA. **(d)** Fluence dependence of LDI ion yield from EBT and NAPA for 5 fmol neurotensin.

DISCUSSION

- To explore the possibility of LDI-MS imaging from NAPA, coronal mouse brain sections were mapped and several metabolites and lipids were located in distinct regions of the brain (Figure 2). Over 75 ions were found to be localized to specific regions.
- For example the lipid ST(24:1) and PE(O-18:2/18:1) were localized in the CC and anterior commissure, whereas PE(18:0/20:4) and PE(36:4) were detected in the CP (Figure 2b and 2c).
- Mouse kidney was imaged using LDI-MS from NAPA. Here the lipid PA(18:1/16:0) and the ion *m/z* 539.2683 were present at higher ion intensities in the renal cortex and the medulla, respectively. The renal vein and artery were discerned by the presence of heme b (Figure3).
- In LDI-MS imaging from NAPA, ion signal from small cell populations exhibited proportionality to the number of cells present (Figure 4d). This enables the study of cellular clusters differing in size and location.
- Fluence dependence of $P_{14}R$ fragmentation for LDI-MS was studied from EBT and NAPA. At low fluences, EBT antennas yielded diverse *a* and *y* fragments, whereas only the parent ion was present for NAPA. As fluence increased, NAPA also produced *a* and *y* fragments (Figure 5a and 5b).
- For small molecule analysis, EBT showed a lower limit of detection than NAPA. (Figure 5c).

CONCLUSIONS

- Overall LDI-MS from NAPA has shown promise for molecular imaging of biological tissue sections with a potential for future drug distribution studies.
- Improving spatial resolution in the imaging of small cell populations by LDI-MS from NAPA can bridge the gap between tissue imaging and single cell analysis.
- Close to threshold fluences, enhanced ultra-trace analysis can be achieved by EBT. Fragmentation patterns can be altered by nanostructure design.

ACKNOWLEDGEMENTS

The authors acknowledge financial support from the Chemical Sciences, Geosciences and Biosciences Division, Office of Basic Energy Sciences, Office of Science, U.S. Department of Energy (Grant DE-FG02-01ER15129) and the GW Selective Excellence Fund. Mouse tissue samples were kindly provided by Dr. J. Nazarian of CNMS.

REFERENCES

[1] Walker, B. N.; Stolee, J. A.; Vertes, A. *Anal. Chem.* **2012**, *84*, 7756.